JOURNAL OF PROPULSION AND POWER
Vol. 25, No. 1, January–February 2009

Thermoanalytical Screening of Nitrogen-Rich Compounds for Ballistic Requirements of Gun Propellant

R. S. Damse,* N. H. Naik, M. Ghosh, and A. K. Sikder
High Energy Materials Research Laboratory, Pune 411 021, India

DOI: 10.2514/1.35789

This study reports the suitability of nitrogen-rich compounds for gun-propellant formulations in regard to flame temperature and burning-rate characteristics. Nine different nitrogen-rich compounds [guanidinium nitrate, triaminoguanidinium nitrate, triaminoguanidinium azide, guanidinium azotetrazolate, triaminoguanidinium azotetrazolate, hydrazinium azotetrazolate, 3, 3'-azobis (6-amino-1, 2, 4, 5-tetrazine), 3, 6-dihydrazino-1, 2, 4, 5-tetrazine, and guanidinium-5-aminotetrazolate] have been studied on the basis of gas-phase thermal analysis to investigate the decomposition pathways. The decomposition mechanism as elucidated for each nitrogen-rich compound has been examined, discussed, and contrasted with an aim to identify the suitable candidates favoring the lower-burning-rate characteristics for the gun-propellant formulations. The suitability has been validated on the basis of closed-vessel testing of selected nitrogen-rich compounds from the preceding.

Nomenclature

α = pressure exponent
β_1 = linear burning-rate coefficient

I. Introduction

IT IS a reported fact that the incorporation of energetic nitrogen-rich compounds into solid gun propellant decreases the flame temperature effectively without affecting the level of force constant [1–4]. This is mainly because, unlike conventional energetic materials, they derive their energy from the combination of higher heats of formation and generation of a large volume of gases (mainly nitrogen). The availability of a large number of C–N and N–N bonds and a low percentage of carbon and hydrogen in these compounds has quadruple positive effects: 1) enhancement of density, 2) need of less oxygen during combustion, in comparison with conventional high-energy materials, 3) formation of low-molecular-weight combustion products, and 4) higher value for the ratio of specific heat of gases [5]. Moreover, the propellant combustion gases rich in nitrogen act to renitride bore surfaces during firing and inhibit erosive surface reactions [6]. The lowered hydrogen concentration in the combustion gas of some of the propellants may also reduce hydrogen-assisted cracking of the bore surface [7]. In view of these versatile characteristics, nitrogen-rich compounds have received major attention from the gun-propellant community [8].

However, the latest experimental studies indicate that the gun propellants containing the triaminoguanidinium salts triaminoguanidinium nitrate (TAGN) and triaminoguanidinium azide (TAGAZ) undergo fast burning, exhibiting higher values for pressure exponent α and linear burning-rate coefficient β_1 [9,10]. The burning-rate characteristics β_1 and α are important parameters in determining the combustion behavior and suitability of a propellant for gun ammunition. The higher value of β_1 (more than 0.15 cm/s/MPa) necessitates an increase in the web size of the propellant grain, which in turn will pose problems in the manufacturing, loadability, and brittle fracture of the grain. Similarly, a higher magnitude of α (more than unity) leads to an exponential rise in burning rate and pressure, which affects the safety of the gun.

Received 21 November 2007; accepted for publication 10 September 2008. Copyright © 2008 by the American Institute of Aeronautics and Astronautics, Inc. All rights reserved. Copies of this paper may be made for personal or internal use, on condition that the copier pay the $10.00 per-copy fee to the Copyright Clearance Center, Inc., 222 Rosewood Drive, Danvers, MA 01923; include the code 0748-4658/09 $10.00 in correspondence with the CCC.

*rdamse@yahoo.co.in (Corresponding Author).

Hence, to achieve the desired values of β_1 and α for the propellant, a few nitrogen-rich compounds representing different structures in their molecular skeleton have been studied in this paper. The compounds were analyzed by thermogravimetry (TG), differential thermal analysis (DTA), thermogravimetry–Fourier-transform infrared (TG-FTIR), and pyrolyser–gas-chromagraphy–mass-spectrometry (Py-GC-MS) techniques with an aim to find the decomposition pathways favorable for these parameters of the gun propellant. Thermal analyses carried out by DTA and TGA experiments spell out the information related to the energy release of a nitrogen-rich compound, whereas the hyphenated techniques such as TG-FTIR and Py-GC-MS have been used to find the decomposition gases evolved during the decomposition profile. The total experimental results have been analyzed to trace the decomposition pathways followed by the nitrogen-rich compound. To validate the fact revealed by the instrumental analysis, a few compositions of the gun propellant containing a nitrogen-rich compound have been evaluated on the basis of closed-vessel testing. The experimental results in regard to the burning-rate characteristics have been shown and discussed, with an aim to select the suitable nitrogen-rich compounds for the gun-propellant applications.

II. Experimental

A. Materials

Nine different nitrogen-rich compounds under five different categories were selected for the present study: nitrate derivatives guanidinium nitrate (GN and TAGN); azide derivatives (TAGAZ), azotetrazolates derivatives guanidinium azotetrazolate (GAT), triaminoguanidinium azotetrazolate (TAGAT), and hydrazinium azotetrazolate (HAT); tetrazine derivatives 3,3′-azobis (6-amino-1,2,4,5-tetrazine) (DAAT) and 3,6-dihydrazino-1,2,4,5-tetrazine (DHTz); and tetrazolate derivative guanidinium-5-aminotetrazolate (GA). Guanidinium nitrate was procured, whereas the rest of the eight compounds were synthesized in the laboratory on the lines of the reported procedures [11–17].

B. Instrumental Analysis

The thermal decomposition studies were carried out on a thermogravimetric simultaneous differential thermal analyzer (TG/SDTA) of TA Instruments (model SDT-Q600) with nitrogen gas at 100 ml/min gas flow. The experiments were conducted at the heating rate of 2°C/min. The thermal-degradation products in various stages [i.e., the evolved gases from TG instrument (SDTA851e, Mettler Toledo)] were analyzed by a hyphenated FTIR instrument (Equinox55, Bruker). The pyrolysis experiments were conducted on a CDS-1000 pyroprobe at between 300 and 1100°C

pyrolyzer temperatures. The pyroprobes were attached with a Clarus 500 gas chromagraphy (GC) coupled with a Clarus 500 mass spectrometer by Perkin-Elmer. The separated pyrolyzates were detected and analyzed by a quadrupole detector using electron-impact ionization mode. The fragmented species were identified by using National Institute of Standards and Technology library data.

C. Closed-Vessel Evaluation

Five different gun-propellant compositions based on nitrocellulose (13.1 N%), cyclotrimethylene trinitramine (RDX), dioctyl phthalate (DOP) stabilizer, and a nitrogen-rich compound were formulated and processed by the standard solvent method using acetone and alcohol (70:30) or ethyl acetate [18]. The propellants were made into a multitubular configuration and subjected to closed-vessel firings in a 700 cm^3 high-pressure closed vessel at 0.20 g/cm^3 density of loading for the determination of burning-rate characteristics.

III. Results and Discussion

It has been observed that the structural aspects of nitrogen-rich compounds influence the overall decomposition process. Each compound follows the typical decomposition pathways that are characteristic of its molecular structure. Hence, to identify a suitable candidate for gun-propellant formulations, the compounds were subjected to instrumental analysis. The results from analytical findings have been discussed with an aim to find the nitrogen-rich compounds favoring the lower-burning-rate characteristics for gun-propellant formulations. The experimental findings have been validated on the basis of closed-vessel evaluation of the propellant.

A. Nitrate and Azide Derivatives

To investigate the cause for the fast-burning behavior of triaminoguanidinium salts, thermal-analysis results obtained for TAGN and TAGAZ were compared with that of guanidinium nitrate (Figs. 1–4). As shown in Fig. 1, the TG curve of TAGN consists of a three-stage weight-loss process: the first stage corresponds to the rapid exothermic reaction observed in the DTA curve between 215 and 225°C, corresponding to a 27% weight loss. The second stage corresponds to the slow endothermic reaction between 225 and 300°C, corresponding to a 65% weight loss. The third stage corresponds to the very slow endothermic reaction beyond 300°C, with the weight loss of 8% taking place at higher temperature (greater than 350°C). The endothermic peak at 215°C in the DTA curve is recognized to be caused by melting. The TG-DTA curve for TAGAZ is shown in Fig. 2.

It has been observed that the TG curve consists of a four-stage weight-loss process. The first stage corresponds to the rapid exothermic reaction observed between 90.46 and 143°C, corresponding to a 28.7% weight loss. The second stage corresponds to endothermic melting at 115.13°C followed by an exothermic rapid reaction between 143 and 172°C, corresponding to a 31% weight loss. The third stage corresponds to endothermic decomposition between 172 and 314°C, corresponding to a 24% weight loss. The fourth stage corresponds to very slow endothermic reaction at the higher temperature, with 13% weight loss taking place beyond 500°C. Hence, the decomposition mechanism for TAGAZ has been proposed on the basis of observed decomposition products, which has been further verified on the basis of differential scanning calorimetry (DSC) analysis (Fig. 3). Thus, it must be noted that unlike TAGN, TAGAZ decomposes exothermically at the first stage, indicating the cleavage of HN_3 as supported by FTIR data. However, thereafter, it follows the same route as TAGN: that is, endothermic melting of the products at 115.13°C followed by rapid exothermic decomposition up to 205.15°C, as shown by DTA.

It has been found that the weight fraction of three amino groups within the TAGN molecule is 0.288, which is approximately equal to the observed weight-loss fraction (0.270) at the first-stage decomposition process. Likewise, the weight fractions of hydrazoic acid (HN_3) and three amino groups within the TAGAZ molecule are

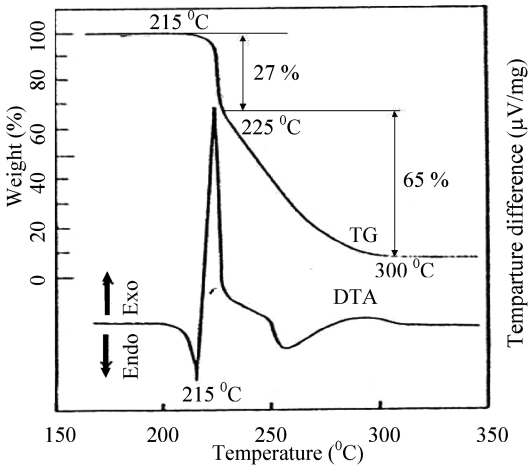

Fig. 1 TG-DTA of TAGN.

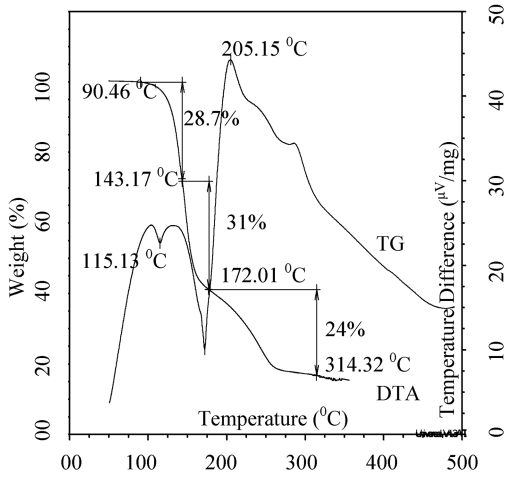

Fig. 2 TG-DTA of TAGAZ.

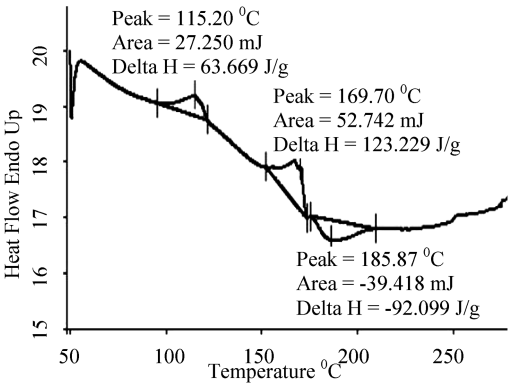

Fig. 3 DSC of TAGAZ.

0.292 and 0.325, which are approximately equal to the observed weight-loss fractions 0.287 and 0.307 at the first and second stages, respectively. This is quite consistent with the possible decomposition pathways followed by TAGN and TAGAZ (Fig. 5). Further supporting evidence to the decomposition pathways has been provided by TG-FTIR and gas-chromagraphy–mass-spectrometry (GC-MS) experiments. The FTIR of the decomposition gases evolved during TG displayed bands within the ranges of 931–966 cm^{-1} and 2235–2363 cm^{-1} and the characteristic mass fragments recorded at $m/z = 17$ and 27 in MS indicate the evolution of NH_3 and HCN, respectively. Evolution of N_2 has also been recorded predominantly in mass spectrometry (MS) ($m/z = 28$) for

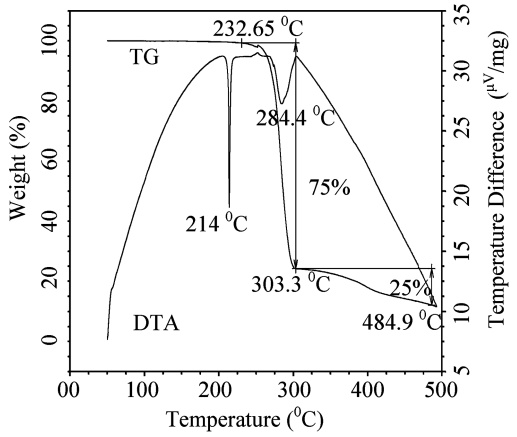

Fig. 4 TG-DTA of GN.

both TAGN and TAGAZ. However, unlike TAGN, an additional FTIR band displayed (2154 cm^{-1}) and the characteristic mass fragment ($m/z = 43$) observed in the case of TAGAZ indicate the evolution of HN_3 (Fig. 5).

Note that the stretching frequencies observed at 1592 cm^{-1} indicate the formation of NH_2 radical, whereas the frequencies at 3528, 3580, and 3653 cm^{-1} correspond to NH species formed after the breakage of the NH_2 radical. The fact has been further confirmed on the basis of mass spectral analysis ($m/z = 16$ and 15 corresponds to NH_2 and NH radicals, respectively). The TG-DTA curve for GN is shown in Fig. 6. The endothermic peak at 214°C in the DTA curve represents the melting point. After melting, a very slow decomposition reaction occurs. The major decomposition of GN begins at 232°C and is completed at 303°C (75% weight loss). The remaining 25% weight fragment decomposes endothermically at higher temperature, as shown in TG. Though GN is similar to TAGN, consisting of the oxidizer fragment (HNO_3) attached to a fuel fragment with an ionic bond (Fig. 6), neither a rapid gasification reaction nor an exothermic reaction occurs. This is in significant contrast to TAGN, as shown in Fig. 1.

The results of our experimental investigations are found in good agreement with the results of thermal analysis of TAGN reported by Kubota et al [19]. The results reveal that the breakage of N-NH_2 bonds available in the molecular structure of TAGN and subsequent reactions are the major source of heat production and not the dissociation of the oxidizer fragment HNO_3 attached by an ionic bond. This indicates that the oxidizer fragment HNO_3 does not contribute to the energy of decomposition. Note that the rapid exothermic reaction observed in the decomposition process represents the nature of energetics for the triaminoguanidinium salts. The exothermic reaction occurs immediately after the endothermic melting. Because the weakest chemical bond available in the molecular skeleton of TAGN and TAGAZ is the N-N bond (159 kJ/mol), the initial bond breakage should take place by the homolytic fission of N-NH_2 bonds producing the highly reactive NH_2 radicals. The energy released by the dissociation of the NH_2 radicals (104.3 kJ/mol) is the heat produced at the early-stage decomposition, which contributes toward the fast burning. In contrast, GN is found to undergo slow exothermic decomposition, attributed to the nonavailability of the facile N-NH_2 bonds in the molecular structure of GN.

B. Azotetrazolate Derivatives

As shown in Fig. 7, the TG curve of GAT consists of a two-stage weight-loss process. The first stage indicates the exothermic rapid reaction observed in the DTA between 200 and 259°C corresponding to 59% weight loss, and the second stage corresponds to the slow endothermic reaction observed beyond 259°C. The first stage denotes the heterocyclic ring opening, which involves abstraction of the acidic protons available in the guanidinium cation by the azotetrazolate anion, which leads to the formation of a highly

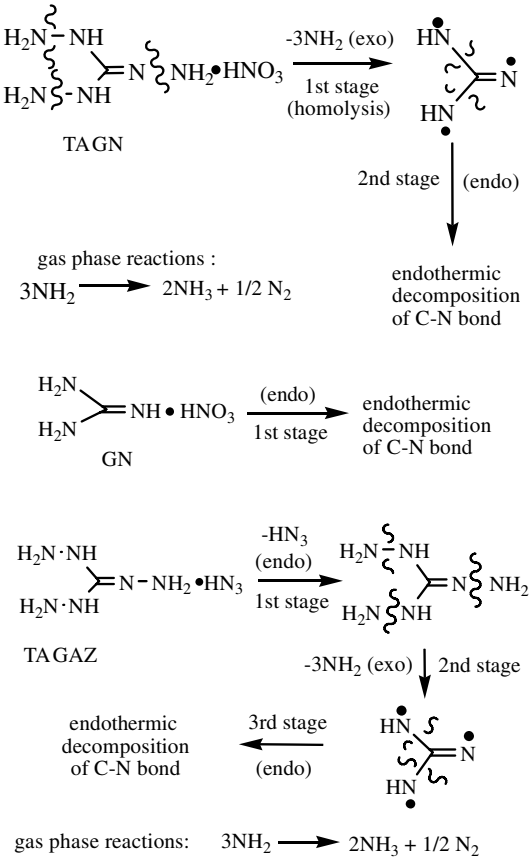

Fig. 5 Possible decomposition pathways for nitrate and azide derivatives.

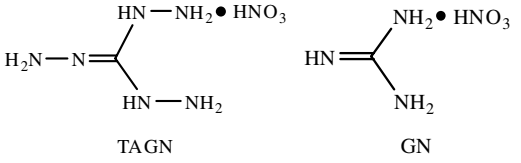

Fig. 6 Chemical structure of TAGN and GN.

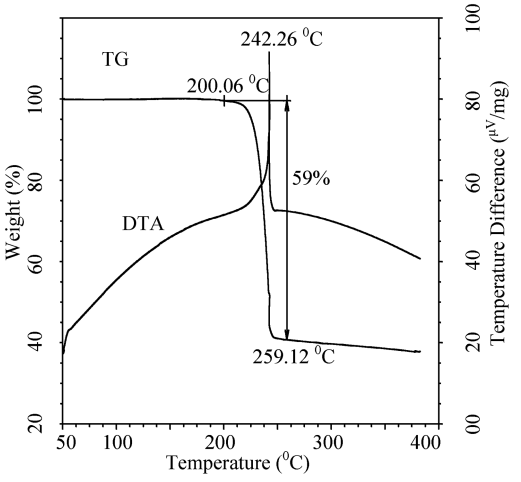

Fig. 7 TG-DTA of GAT.

unstable azotetrazolate cation and subsequent opening of the azotetrazolate ring with the release of molecular nitrogen and cyanamid. Note that the compound has been subjected to pyrolysis at a higher temperature (800°C), which could lead to the transfer of two

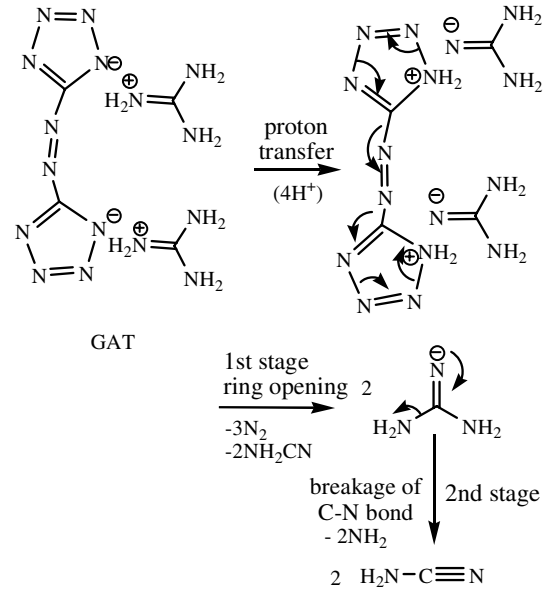

Fig. 8 Decomposition pathways for GAT.

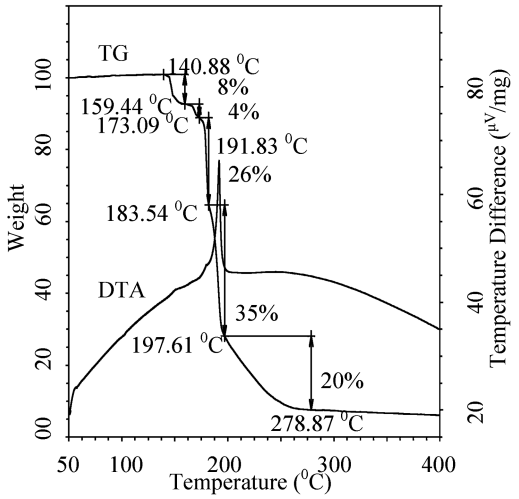

Fig. 9 TG-DTA of TAGAT.

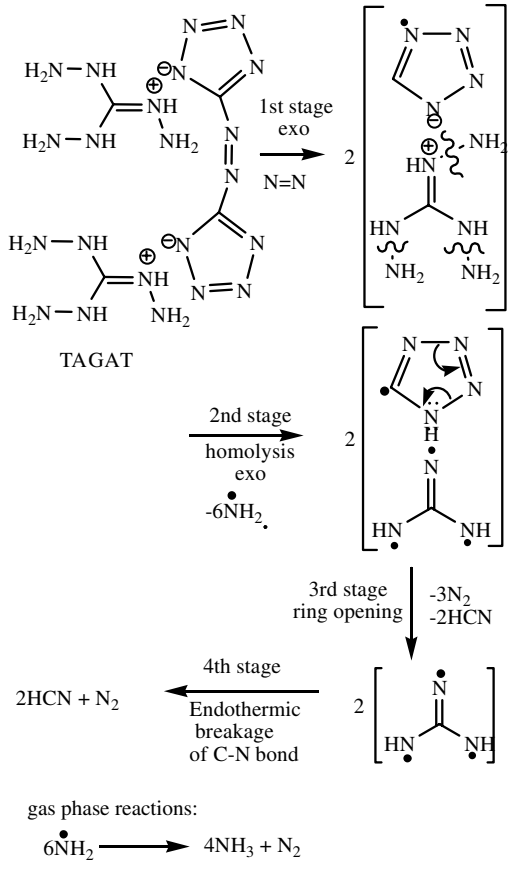

Fig. 10 Decomposition pathways for TAGAT.

protons from the guanidinium cation to the azotetrazolate anion to form the azotetrazolate cation.

After transfer of the first proton from the guanidinium nitrogen, the cation attains a $sp2$ hybridized state, whereas the azotetrazolate nitrogen exists in a $sp3$ hybridized state; therefore, the guanidinium proton is more acidic than the azotetrazolate proton. The theoretical weights of the fractions of $(N_2)_3$ and $(NH_2CN)_2$ within the GAT molecule (0.5900) have been found to be approximately equal to the observed weight loss (0.5881), which is quite consistent with the opening of the azotetrazolate ring (Fig. 8).

The second stage, corresponding to very slow endothermic reaction, indicates the breakage of relatively strong C-N bonds (770 kJ/mol) as compared with N-N bonds (159 kJ/mol). However, TAGAT, a triamino derivative of GAT, follows decomposition pathways with an entirely different mechanism attributed to the introduction of the triamino group. The TG curve of TAGAT reveals a four-stage weight-loss process (Fig. 9). The first stage corresponds to the rapid exothermic reaction observed in the DTA between 141 and 159°C, corresponding to an 8% weight loss; the second stage also corresponds to the rapid exothermic reaction between 173 and 183°C, corresponding to a 26% weight loss; the third stage corresponds to the exothermic decomposition between 183 and 198°C, corresponding to a 35% weight loss; and the fourth stage corresponds to the very slow endothermic reaction between 198 and 279°C, corresponding to a 20% weight loss. However, the 4% weight loss observed between 159 and 173°C has been considered to be due to the entrapped impurities.

The weight loss observed in the first-stage (0.08117), second-stage (0.2622), third-stage (0.3482), and fourth-stage decomposition (0.2033) has been found approximately equal to the theoretical mass of the fractions of $N=N$, $(NH_2)_6$, $(N_2)_3$, and HCN, respectively. This is in good agreement with the decomposition pathways followed by TAGAT (Fig. 10). It is believed that unlike GAT, the azotetrazolate anion in TAGAT is unable to abstract the acidic proton available in the triaminoguanidinium cation because of the steric hindrance caused by the amino group attached to the nitrogen atom carrying an acidic proton. Therefore, it favors the decomposition initiated by the cleavage of the triggered azo group rather than the proton-transfer initiation, as observed in GAT. In contrast, HAT is found to decompose in a single stage. The TG-DTA curve corresponds to the exothermic decomposition observed in DTA between 122.92 and 168.33°C, corresponding to a 77.43% weight loss. However, thereafter, it follows endothermic decomposition resulting from the breakage of relatively strong C-N bonds (Fig. 11). This suggests that the decomposition initiates with the homolytic cleavage of N-NH_2 bonds, followed by exothermic opening of the azotetrazolate ring (Fig. 12).

Further supporting evidence to the decomposition pathways followed by GAT, TAGAT, and HAT has been provided by TG-FTIR and pyrolysis GC-MS experiments on the basis of characteristic FTIR frequencies and mass fragments of the decomposition gases evolved at the different stages of the decomposition profile (Figs. 8, 10, and 12), as mentioned in Sec. III.A

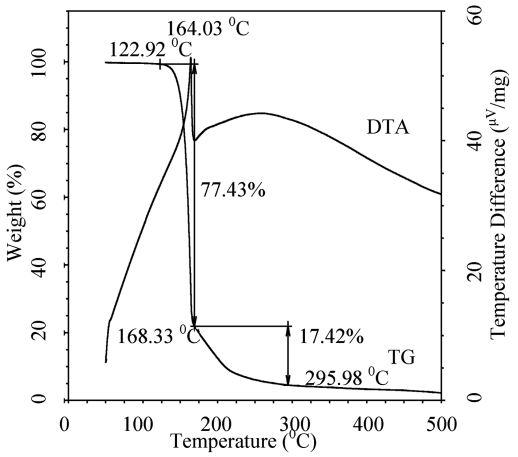

Fig. 11 TG-DTA of HAT.

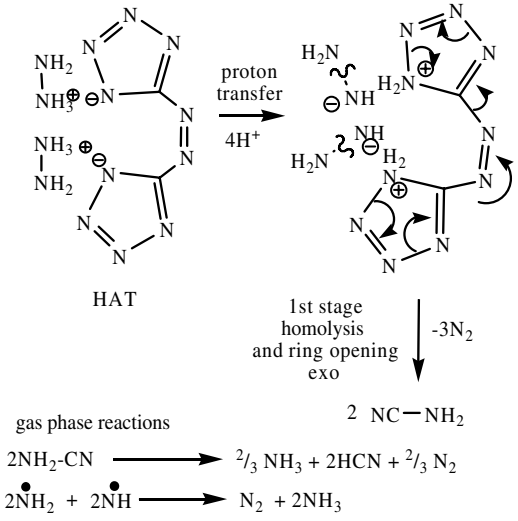

Fig. 12 Decomposition pathways for HAT.

C. Tetrazine Derivatives

The TG curve of DAAT consists of a two-stage weight-loss process (Fig. 13). The first stage corresponds to the exothermic rapid reaction observed in the DTA between 185 and 280°C, corresponding to a 14.28% weight loss, whereas the second stage corresponds to the slow endothermic reaction between 280 and 320°C, corresponding to a 74.09% weight loss. It has been found from the DSC curve that the exothermicity is spread over a relatively narrow temperature range, appearing as a sharp heat flow peak (Fig. 14). Hence, the highest heat release in the first-stage decomposition is considered to be due to the cleavage of the triggered azo group. The weight fraction of N = N within the DAAT molecule is 0.1270, which has been found to be approximately equal to the observed weight-loss fraction (0.1424). This is inconsistent with the exothermic cleavage of the azo group in the first stage (Fig. 15). In contrast, DHTz follows an entirely different pathway that is characteristic of its molecular structure.

The TG curve consists of a three-stage weight-loss process (Fig. 16). The first stage corresponds to the exothermic reaction observed in the DTA between 127.51 and 151.98°C, corresponding to 25.63% weight loss; the second stage corresponds to the relatively slow endothermic reaction between 151.98 and 202.57°C, corresponding to a 18.57% weight loss; and the third stage corresponds to the very slow endothermic reaction between 202.57 and 354.77°C, corresponding to a 26.70% weight loss. It is seen that the theoretical weight fractions of two amino groups is 0.220 and one molecule of nitrogen is 0.1970 within the DHTz molecule, which has been found to be approximately equal to the observed weight loss

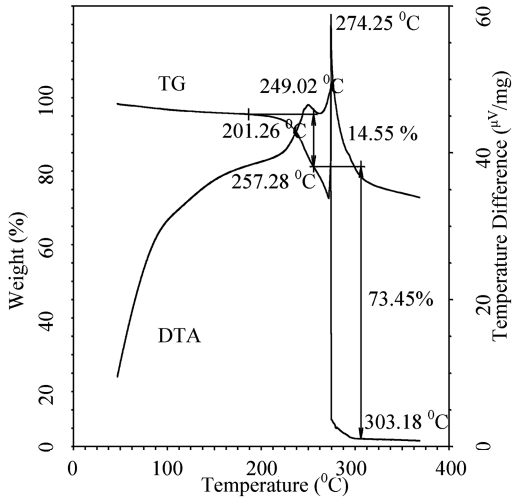

Fig. 13 TG-DTA of DAAT.

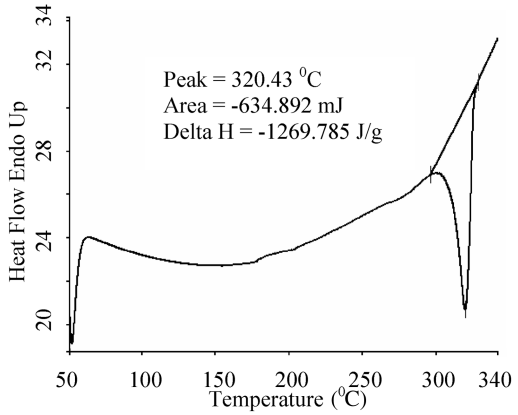

Fig. 14 DSC of DAAT.

0.2563 and 0.1862, respectively, in the first and second stages. This indicates the exothermic decomposition of N-NH_2 bonds followed by endothermic opening of the tetrazine ring (Fig. 17). Further support to the decomposition pathways followed by DAAT and DHTz has been obtained from the TG-FTIR and GC-MS experiments, as discussed with TAGN and TAGAZ in Sec. III.A.

D. Tetrazolate Derivatives

The TG-DTA curve for GA shows an endothermic melting at 124°C, followed by four-stage weight-loss process (Fig. 18). The first stage corresponds to weak exothermic decomposition observed in the DTA between 150 and 231.6°C,; the second and third stages also correspond to weak exothermic decomposition within the temperature range of 231.6 to 357.8°C, corresponding to 15 and 11.6% weight loss, respectively; and the fourth stage corresponds to endothermic decomposition between 357.8 and 560°C, corresponding to 44.1% weight loss. The identification of the decomposition gases allows the evaluation of the chemical processes during the thermal degradation of GA TG-FTIR, and GC-MS identifies HN_3, NH_3, and NH_2-CN as the decomposition gases evolved in the first, second, and third stages of the decomposition process, respectively. However, the appearance of mass fragments at $m/z = 126$ in GC-MS indicate the formation of melamine as an intermediate species in the gas phase (Fig. 19).

The theoretical mass of HN_3 (0.2990) within the GA molecule coincides well with the observed weight loss (0.2930) in the first stage. This is consistent with the evolution of HN_3. The release of HN_3 in the first stage denotes the ring opening of heterocyclic tetrazolate, which leads to the formation of residue components (viz., guanidine and cyanamid). The evolution of ammonia corresponding

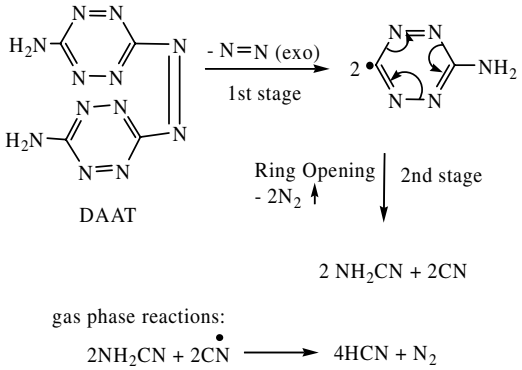

Fig. 15 Decomposition pathways for DAAT.

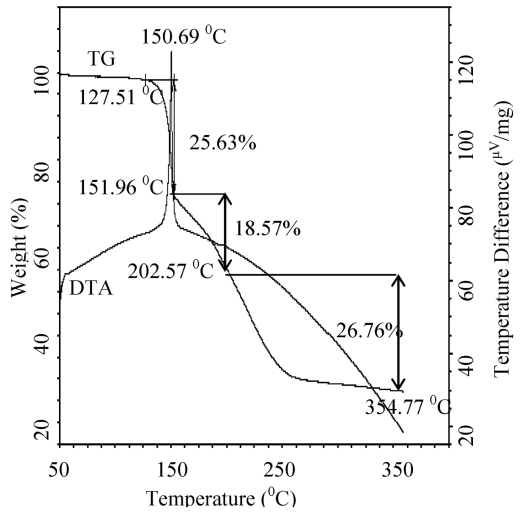

Fig. 16 TG-DTA of DHTz.

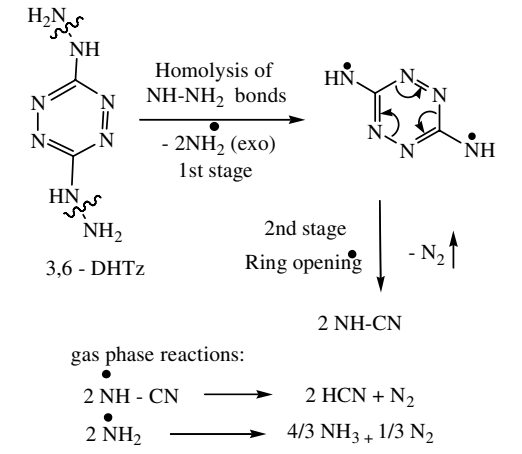

Fig. 17 Decomposition pathways for 3, 6-DHTz.

to a mass loss of 0.1160 in the second stage has been verified on the basis of its theoretical mass (0.1180) within the GA molecule. This indicates that the simultaneous reactions must be taking place among the residue components, forming a thermally stable intermediate species such as melamine (Fig. 19). The formation of melamine has been considered as significant evidence to the decomposition pathways followed by GA.

It is seen that the decomposition pathways followed by each nitrogen-rich compound have been influenced by its molecular structure. The compounds undergoing decomposition with the rapid exothermic reactions exhibit fast-burning behavior (e.g., TAGN, TAGAZ, DHTz, TAGAT, HAT, and DAAT), whereas those undergoing decomposition with the slow exothermic reactions favor slow-burning behavior (e.g., GN and GA). To validate the fact, four different gun-propellant compositions based on TAGN, TAGAZ, GN, and GA have been evaluated on the basis of a closed-vessel test and the results are compared with that of the control composition (Table 1). The results indicate that all the propellants containing the nitrogen-rich compounds exhibit lower flame temperatures with only a marginal decrease in force constant. However, the propellants containing triaminoguanidinium salts (TAGN and TAGAZ) exhibit higher-burning-rate characteristics ($\alpha = 1.40$ and $\beta_1 = 0.30$ cm/s/MPa), which indicates the nonsuitability of the propellant for gun applications, whereas the propellants containing GN and GA show reasonably lower-burning-rate characteristics and are thus suitable for gun applications.

A higher burn rate is attributed to homolytic fission of N-NH_2 bonds in the molecular structure of TAGN and TAGAZ producing highly unstable and reactive amino (NH_2) radicals. The energy released by the dissociation of NH_2 radicals is the main source of heat produced at an early stage of the decomposition process, and the

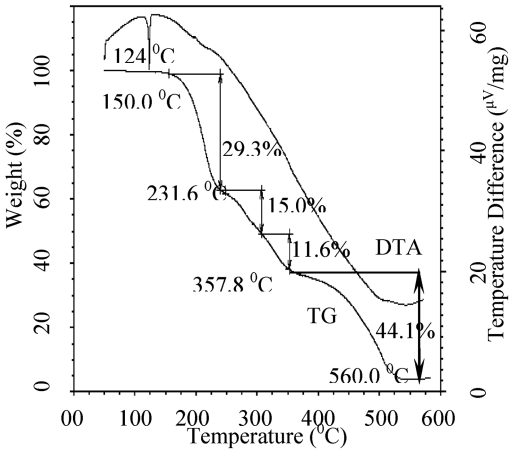

Fig. 18 TG-DTA of GA.

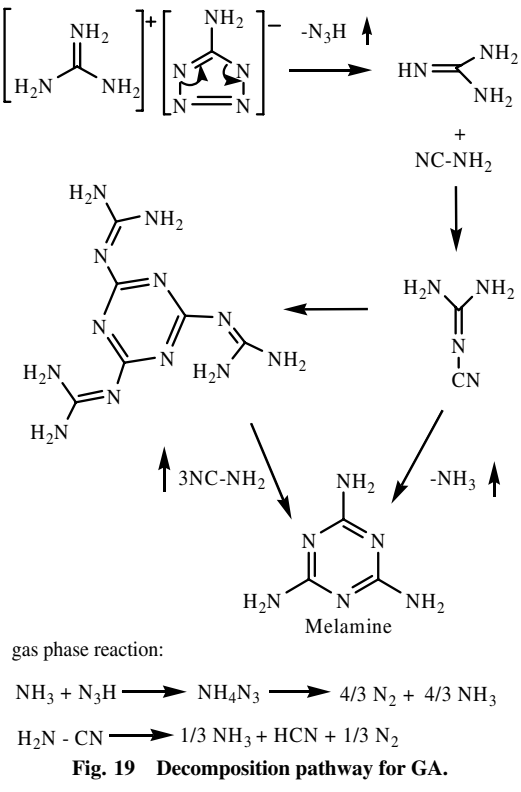

Fig. 19 Decomposition pathway for GA.

Table 1 Closed-vessel results of the propellants containing nitrogen-rich compound

Serial no.	Propellant composition				Force constant, J/g	Flame temperature, K	Linear burning-rate coefficient β_1, cm/s/MPa	Pressure exponent α
	NC (13.1 N%)	RDX	DOP	Carbamite				
1	28	65	6	1	1200	3210	0.14	0.84
2 (**TAGN** = 15)	28	50	6	1	1163	2900	**0.30**[a]	**1.40**[a]
3 (**TAGAZ** = 15)	28	50	6	1	1158	2850	**0.30**[a]	**1.40**[a]
4 (GN = 15)	28	50	6	1	1118	2915	0.13	0.80
5 (GA = 15)	28	50	6	1	1160	2870	0.15	0.95

[a]TAGN- and TAGAZ-based propellants exhibit unacceptably higher values for β_1 and α, as shown in bold.

same contributes toward the enhancement in burning-rate characteristics. It is a known fact that decomposition of an explosive material depends upon the generation of free radicals, which forms the nucleus of the chain process, and hence the materials that help in the generation of free radicals or the removal of a barrier in their generation would lower the activation energy [20]. In contrast, GN and GA are found to undergo a slow decomposition process and thus exhibit slow-burning-rate behavior.

It has been observed that GN decomposes with an endothermic melting followed by very slow exothermic reactions. This is attributed to slow breakage of the relatively strong C-N bonds available in its molecular structure. Likewise, GA also decomposes with the slow exothermic reactions exhibiting the lower-burning-rate characteristics as found in the closed-vessel evaluation (Table 1). The ring-opening mechanism has been predicted on the basis of evolution of HN_3, and the slow decomposition behavior is attributed to the formation of thermally stable cyclic azines such as melamine [21]. It is reported that the melamine and its higher homologs (melam, melem, and melon) retard the heat and mass transfer rates at the surface of the propellant and thus act as burning-rate modifiers [22]; that is why the propellant based on GA exhibits lower-burning-rate characteristics. The similar pattern of decomposition behavior exhibited by GN and GA has been well demonstrated on the basis of DTA profiles (Figs. 4 and 18).

In the case of the azotetrazolate derivatives such as TAGAT, the net heat output produced by the cleavage of the triggered azo group and the homolytic fission of N-NH_2 bonds contributes toward the rapid exothermic decomposition (Fig. 9). HAT also exhibits more or less similar decomposition behavior resulting from the homolytic fission of N-NH_2 bonds, followed by exothermic opening of the azotetrazolate ring with the evolution of molecular nitrogen (Fig. 11). In contrast, GAT does not contain N-NH_2 bonds in its molecular structure and exhibits rapid exothermic decomposition because of the exothermic opening of the azotetrazolate ring with the evolution of molecular nitrogen (N_2).

It is reported that the ring-opening mechanism taking place with the release of molecular nitrogen leads to generating higher heat output. Hence, GAT also decomposes with rapid exothermic reaction, as shown by the DTA (Fig. 8). Tetrazine derivatives such as DAAT and DHTz are found to undergo rapid exothermic decomposition because of the exothermic cleavage of the triggered azo group in DAAT and homolytic fission of N-NH_2 bonds in DHTz. Moreover, both DAAT and DHTz decompose via the opening of the heterocyclic ring with the evolution of nitrogen gas that further contributes toward the exothermicity. Thus, the decomposition mechanism followed by the azotetrazolate and tetrazine compounds favors the fast-burning behavior. However, the compounds need to be evaluated for a gun-propellant formulation.

IV. Conclusions

Out of nine nitrogen-rich compounds in the experiment, it can be concluded that the rapid exothermic decomposition of nitrogen-rich compounds such as TAGN, TAGAT, HAT, DAAT, and DHTz is responsible for the higher value of burning-rate characteristics α and β_1. The compounds such as GA and GN undergo slow exothermic decomposition that favor the lower values of burning-rate characteristics of propellant. The lowering of burning-rate characteristics can be attributed to the decomposition mechanism of GA that takes place via the opening of the heterocycle with the formation of hydrazoic acid and melamine as the decomposition species. On the other hand, the nonavailability of facile N-NH_2 bonds in the molecular structure of GN is an attribute for the lower-burning-rate characteristics of the gun propellant. Thus, the data generated out of experimentation accomplished in this paper can be better input to augment the suitability of guanidinium nitrate and guanidinium-5-aminotetrazolate as nitrogen-rich compounds for future gun-propellant formulations.

Acknowledgment

The authors are thankful to A. Subhanada Rao, Director of the High Energy Materials Research Laboratory (HEMRL), for his constant encouragement.

References

[1] Flanagan, J., Haury, E., and Vernon, E., "Cool Burning Gun Propellants Containing Triaminoguanidinium Nitrate and Cyclo-Tetramethylene Tetranitramine with Ethyl Cellulose Binder," U.S. Patent 3,909,323, Sept. 1975.

[2] Flanagan, J., Haury, E., and Vernon, E., "Gun Propellants Containing Nitroguanidine," U.S. Patent 4,373,976, Feb. 1983.

[3] Flanagan, J., Haury, E., and Vernon, E., "Gun Propellants," U.K. Patent 1,432,327, 14 Apr. 1976.

[4] Haury, Vernon, Frankel, and Milton, "Triaminoguanidinium Nitrate Containing Gun Propellants," Canada Patent 977,154, Nov. 1974.

[5] Simmons, R. L., "Guidelines of High Energy Gun Propellants," *27th International Conference of ICT on Energetic Materials*, Fraunhofer Inst. fur Chemische Technologie, Karlsruhe, Germany, 1996, pp. 22.01–22.16.

[6] Chavez, D. E., and Hiskey, M. A., "1, 2, 4, 5-Tetrazine Based Energetic Materials," *Journal of Energetic Materials*, Vol. 17, No. 4, 1999, pp. 357–377. doi:10.1080/07370659908201796

[7] Niklas, W., and Nilolaj, V., "Triaminoguanidinium Dinitramide, TAGDN: Synthesis and Characterization," *Propellants, Explosives, Pyrotechnics*, Vol. 28, No. 6, 2003, pp. 314–318. doi:10.1002/prep.200300022

[8] Loebbecke, S., Pfeil, A., and Krause, H., "Thermoanalytical Screening of Nitrogen-Rich Substances," *Propellants, Explosives, Pyrotechnics*, Vol. 24, No. 5, 1999, pp. 168–175. doi:10.1002/(SICI)1521-4087(199906)24:03<168::AID-PRE-P168>3.0.CO;2-0

[9] Damse, R. S., Omprakash, B., Yevale, A. D., and Singh, A., "Evaluation of Triaminoguanidinium Salts for Solid Gun Propellant," *Proceedings of the 5th International High Energy Materials Conference and Exhibit*, High Energy Materials Society of India, High Energy Materials Research Lab., Pune, India, Nov. 2005.

[10] Damse, R. S., and Redkar, A. S., "High Impetus Cool Burning Gun Propellants," *Defence Science Journal*, Vol. 50, No. 3, 2000, pp. 281–288.

[11] Earl, T., and Niles, "Triaminoguanidinium Azide," U.S. Patent 3,321,494, May 1967.

[12] Chavez, D. E., and Hiskey, M. A., "1,2,4,5-Tetrazine Based Energetic Materials," *Journal of Energetic Materials*, Vol. 17, No. 6, 1999, pp. 357–377. doi:10.1080/07370659908201796

[13] Chevez, D. E., Hiskey, M. A., and Gilardi, R. D., "3, 3′-Azobis (6-amino-1, 2, 4, 5-tetrazine) A Novel High Nitrogen Energetic Material," *Angewandte Chemie International Edition*, Vol. 39, No. 10, 2000,

pp. 1791–1793.
doi:10.1002/(SICI)1521-3773(20000515)39:10<1791::AID-ANIE1791>3.0.CO;2-9

[14] Hiskey, M. A., Goldman, N., and Stine, J. R., "High Nitrogen Energetic Materials Derived from Azotetrazolate," *Journal of Energetic Materials*, Vol. 16, Nos. 2–3, 1998, pp. 119–127.
doi:10.1080/07370659808217508

[15] Peng, Y. L., and Wong, C. W., "Preparation of Guanidinium Azotetrazolate," U.S. Patent 5,877,300, Mar. 1999.

[16] Hammerl, A., Klapotke, T. M., Noth, H., Warchhold, M., Holl, G., Kasier, M., and Ticmanis, W., "$[N_2H_5] + {}_2[N_4C - N = N - CN_4]^{2-}$: A New High-Nitrogen High-Energetic Material,"*Inorganic Chemistry*, Vol. 40, 2001, pp. 3570–3575.
doi:10.1021/ic010063y

[17] Jochen, N., Otto, G., Stephan, S., Heike, S., and Wenka, S., "Synthesis, Characterization and Thermal Behavior of Guanidinium-5-Aminotetrazolate (GA): A New Nitrogen Rich Compound," *Propellants, Explosives, Pyrotechnics*, Vol. 28, No. 4, 2003, pp. 181–188.
doi:10.1002/prep.200300003

[18] Singh, S., "Double Base Propellants," Controllerate Inspection of Military Explosives, Rept. 1/76, Pune, India, 1976, p. 124.

[19] Kubota, N., Hirata, N., and Sakamoto, S., "Decomposition Chemistry of TAGN," *Propellants, Explosives, Pyrotechnics*, Vol. 13, No. 3, 1988, pp. 65–68.
doi:10.1002/prep.19880130302

[20] Dhar, S. S., "Composite Modified Double Base Propellant Based on Energetic Azidopolymer-GAP," Ph.D. Thesis, Univ. of Poona, Pune, India, 1993.

[21] Brill, T. B., and Ramanathan, H., "Thermal Decomposition of Energetic Materials: Chemical Pathways That Control the Burning Rate of 5-Aminotetrazolate and Its Hydro Halide Salts," *Combustion and Flame*, Vol. 122, Nos. 1–2, 2000, pp. 165–171.
doi:10.1016/S0010-2180(00)00111-5

[22] Stoner, C. E., and Brill, T. B., "Thermal Decomposition of Energetic Materials of Melamine-Like Cyclic Azines as Mechanism for Ballistic Modification of Composite Propellants by DCD, DAG and DAF," *Combustion and Flame*, Vol. 83, Nos. 3–4, 1991, pp. 302–308.
doi:10.1016/0010-2180(91)90077-O

S. Son
Associate Editor